Propensity of Human Embryonic Stem Cell Lines During Early Stage of Lineage Specification Controls Their Terminal Differentiation into Mature Cell Types

Rajarshi Pal,* Swapnil Totey,† Murali Krishna Mamidi,† Vijay S. Bhat,‡ and Satish Totey†,[1]

*Manipal Institute of Regenerative Medicine, Manipal University Branch Campus, Bangalore 560071, India; †Stempeutics Research Malaysia Sdn. Bhd, Bukit Jalil, 57000 Kuala Lumpur, Malaysia; and ‡Department of Biochemistry, Manipal Hospital Diagnostic Services, Manipal Hospital, Bangalore 560017, India

Human embryonic stem cells (hESCs) are able to stably maintain their characteristics for an unlimited period; nevertheless, substantial differences among cell lines in gene and protein expression not manifested during the undifferentiated state may appear when cells differentiate. It is widely accepted that developing an efficient protocol to control the differentiation of hESCs will enable us to produce adequate numbers of desired cell types with relative ease for diverse applications ranging from basic research to cell therapy and drug screening. Hence of late, there has been considerable interest in understanding whether and how hESC lines are equivalent or different to each other in their in vitro developmental tendencies. In this study, we compared the developmental competences of two hESC lines (HUES-9 and HUES-7) at molecular, cellular and functional levels, upon spontaneous differentiation without any added inducing agents. Both cell lines generated the three embryonic germ layers, extra-embryonic tissues and primordial germ cells during embryoid body (EB) formation. However HUES-9 showed a stronger propensity towards formation of neuroectodermal lineages, whereas HUES-7 differentiated preferentially into mesoderm and endoderm. Upon further differentiation, HUES-9 generated largely neural cells (neurons, oligodendrocytes, astrocytes and gangliosides) whereas HUES-7 formed mesendodermal derivatives, including cardiomyocytes, skeletal myocytes, endothelial cells, hepatocytes and pancreatic cells. Overall, our findings endorse the hypothesis that independently-derived hESCs biologically differ among themselves, thereby displaying varying differentiation propensity. These subtle differences not only highlight the importance of screening and deriving lines for lineage-specific differentiation but also indicate that individual lines may possess a repertoire of capabilities that is unique. Exp Biol Med 234:1230–1243, 2009

Key words: human embryonic stem cell lines; pluripotency; spontaneous differentiation; embryoid body; neuroectoderm; mesendoderm; propensity; characterization; marker expression

Introduction

Since the first establishment of human embryonic stem cells (hESCs) (1), several attempts have been made to direct them to produce specific cell types (2). hESCs while demonstrating unlimited proliferation in culture generally retain a normal karyotype and strongly express pluripotency genes, including Oct-4, Nanog, Sox-2, Rex-1 and cell surface antigens such as SSEA-3, SSEA-4, TRA-1–60 and TRA-1–81. They also demonstrate high levels of telomerase activity and are capable of giving rise to a myriad of somatic cell types both in vivo and in vitro (3). Owing to their true differentiation potential hESCs are considered as the best potential source of cells for cell replacement therapies. Nevertheless, the fact that they form heterogeneous populations of various cell types thwarts their utility as sources of individual cell types.

To date many protocols have been perceived with the aim of inducing the differentiation of hESCs into desired cell types. At the same time it has been documented that different hESC lines have different outcomes under identical

This work was supported in part by Department of Biotechnology, Govt. of India, Manipal University, Madhav Nagar, Manipal, India and Stempeutics Research Private Limited, Bangalore, India.

[1] To whom correspondence should be addressed at Stempeutics Research Malaysia Sdn. Bhd., Lot 3-I-7, Enterprise 4, Technology Park Malaysia, Bukit Jalil, Kuala Lumpur, 57000 Kuala Lumpur, Malaysia. E-mail: satish.t@stempeutics.com.my

Received January 29, 2009.
Accepted May 20, 2009.

DOI: 10.3181/0901-RM-38
1535-3702/09/23410-1230$15.00

culture conditions (4–6); similar results have been obtained with mouse ESCs (7). These differences indicate that factors other than culture conditions and passage numbers must be taken into account while studying differentiation of hESCs. Since ES cell lines are derived from individual embryos, they are likely to possess unique characteristics. In fact recent studies focusing on epigenetic signature of different hESC lines have clearly indicated that individual cell lines may have distinct line-specific epigenetic profiles (8–10) which might eventually influence their differentiation properties. Further adaptation to distinct cell culture conditions may instigate selection pressure altering the characteristics of the cell lines at the epigenetic or chromosomal level. Although there are plenty of reports about differentiation of hESC into a variety of cell types, only a few studies address the differences between individual cell lines and they are largely focused on transcriptional profiling (11–13). Although these studies have indicated that the mRNA expression patterns diverge to some extent between the hESC lines, biological significance of the variation has not been studied in detail.

However, other than intrinsic factors, several other parameters may have an influence on the lineage commitment of differentiating hESCs into representatives of three germ layers: ecto-, meso- and endoderm including trophectoderm. The method of handling (passaging) and status of the input hESC population, age of the cell line, media composition and the method of inducing differentiation can affect the fate of differentiating hESCs (14). hESC propagation typically requires paracrine and autocrine signaling via secreted factors as well as physical contact via cell-surface adhesion molecules and gap-junction mediated intercellular coupling (15, 16). Partial dissociation of hESC colonies, which is commonly practiced, results in a wide range of colony and aggregate (embryoid body, EB) sizes. This presents a potential source of variability in subsequent differentiation experiments (17). Notably, a better control over human EB size has been reported by a number of groups using forced aggregation of defined cell numbers (18, 19). EB size may not only be a critical parameter to improve reproducibility of hESC differentiation but also a potentially important component to regulate endogenously controlled cell type-specific differentiation, as reported recently (20). However, the role of developmentally controlled EBs on endogenously driven tissue-specific differentiation has not been explored much.

Since relatively little is known about dissimilarities in developmental competencies between hESC lines, we sought to investigate this question in the present study. We examined propensity of HUES-7 and HUES-9 lines via spontaneous differentiation during EB formation without addition of growth factors to minimize any bias towards differentiation. We compared the differentiation propensities of two hESC lines at three stages of differentiation: i) in the undifferentiated state, ii) at the time of EB formation and iii) after terminal differentiation into mature cell types. Further, in order to comprehend our preliminary results we performed quantitative analysis of the cells at transcription level, protein synthesis and enzyme activity. Our findings suggest that individual hESC lines can not only differ in their early differentiation propensities but such differences are retained through the course of terminal differentiation into matured cell types.

Materials and Methods

Culture and Expansion of hESCs. HUES-9 and HUES-7 cell lines were cultured on mitomycin-C treated CF1 mouse derived embryonic feeder (MEF) cells at 37°C, 5% CO_2 in ES media consisting of 80% KO DMEM, 20% Knockout serum replacement, 2 mM L-Glutamine, 1% non essential amino acid solution, 0.1 mM β-mercaptoethanol, 4 ng/ml human basic FGF-2 and 50 U/ml penicillin-streptomycin (all from Invitrogen, CA, USA). Medium was changed every alternate day and the cells were passaged every 4–5 days in order to maintain them at undifferentiated state. hESC colonies were subjected to mild trypsinization with Trypsin-EDTA (0.05%; Invitrogen) during regular propagation.

Karyotyping. Karyotype examination of hESCs cultured on MEFs was performed at every 5 passages for both the cell lines during the study. Cells were treated with Colcemid (Sigma) for metaphase arrest, fixed in Carnoy's fixative and chromosome spreads were visualized by standard Giemsa-banding procedure. More than 200 cells were analyzed per cell line at any time point and reported according to the International System for Human Cytogenetic Nomenclature.

EB Formation. For induction of EB formation the hESCs were seeded on 60 mm bacteriological petri dishes (BD Biosciences) containing ES media without FGF2. At a time, semi-confluent hESCs from three confluent 35-mm dishes were harvested by trypsinization and used for inducing EB production. The EBs formed were screened for typical round morphology under an inverted microscope (NIKON). On day 2.5 EBs were collected and washed thrice in culture media and finally transferred to fresh media. This step was carried out to dispose of the dying MEFs and also to select the morphologically similar healthy EBs.

Spontaneous Differentiation of hESCs. hESC aggregates (EBs) were cultured in suspension for 8–10 days in hESC differentiation medium, containing KO-DMEM (Invitrogen), 20% Knock-Out Serum (Gibco), 100 μM non essential amino acids, 2 mM Glutamax (Invitrogen) and 100 μM β-mercaptoethanol followed by plating onto freshly prepared 0.1% matrigel (BD Biosciences) coated tissue culture dishes. Day 2 onwards, the plated EBs started forming outgrowths in static cultures. With progressive days in differentiation (days 14–21), the sprouting EBs developed into a lawn of heterogeneous cells clearly distinguishable from undifferentiated hESCs.

Total RNA Isolation, cDNA Synthesis and Semi-Quantitative PCR. Total RNA from cell pellets collected at different time points was isolated using TRIZOL reagent (Invitrogen) as per the manufacturer's protocol. cDNA was synthesized using Superscript III First Strand Synthesis system (Invitrogen) as per the manufacturer's instructions. PCR was carried out using IU Taq DNA Polymerase (Sigma) and $MgCl_2$ to a final concentration of 1.5 mM in a total volume of 25 μl/reaction. GAPDH was used as the housekeeping gene control. PCR cycles consisted of initial denaturation at 95°C for 5 minutes followed by 30–35 amplification cycles of denaturation at 94°C for 45 seconds, annealing for 45 seconds, and extension at 72°C for 45 seconds and final extension at 72°C for 10 minutes. The RT-PCR primers, amplicon sizes and their annealing temperatures were similar to reference 33.

Quantitative Real-Time PCR. Pre-designed Assays on Demand TaqMan® probes and primers were procured from Applied BioSystems. Total RNA was extracted from undifferentiated hESCs and EBs and reverse transcribed using Superscript III (Invitrogen). qRT-PCR analysis was performed using ABI PRISM 7500 Sequence Detection System (Applied BioSystems). After an initial denaturation for 10 minutes at 95°C, the reaction was run for 40 cycles of PCR (95°C for 15 seconds, 60°C for 1 minute). Changes in gene expression (in triplicates) were normalized to 18S rRNA levels in terms of fold change.

Indirect Immunofluorescence. To check the immunoreactivity of the EBs and their differentiated progenies to a set of key markers indicating early differentiation and tissue formation, cells were fixed in 4% paraformaldehyde for 10 minutes at room temperature followed by two PBS washes. Upon fixing the cells, permeabilization was done with 0.01% Triton X-100 for 10 minutes. After blocking with 3% BSA/PBS, the cells were probed with primary antibodies overnight at 4°C. The following primary antibodies were used in the study: Brachyury, Ventricular myosin heavy chain-β, MyoD, Nestin, β-III tubulin, A2B5, K3/12, AFP, Insulin and Albumin (all from Chemicon, USA, except AFP). The cells were then washed and incubated with appropriate secondary antibodies at room temperature for 1.5 hours. Finally the cells were counter stained with 4′,6-diamidino-2-phenylindole dihydrochloride (DAPI) (Vector Laboratories, Inc., Burlingame, CA). Fluorescence images were captured and analyzed using a NIKON ECLIPSE 90i microscope (NIKON Corporation, Japan) and Image Pro Express Software (Media Cybernetics, Inc., MD, USA). The negative controls were processed without primary antibody.

EB Sectioning, Histopathology and Immunohistochemical Analysis by Tri-Color Staining. hESC aggregates were formed and healthy looking roundish comparatively larger EBs were harvested at days 8–10 in culture for immunohistological examination. This experiment was carried out in order to acquire a better insight into the localization of particular lineage/tissue specific proteins within the three-dimensional EBs. Samples were fixed in formalin for 20 minutes. Fixed samples were dehydrated in a series of graduated alcohol solutions (30%–100%) followed by xylene. The EBs were later embedded in paraffin after incubating in a combination of paraffin and xylene, respectively, for 30 minutes in each solution (1:3, 1:1 and 3:1). 5–6 μm paraffin sections were cut using a rotary microtome. After keeping for 24 hours on a 37°C hot plate, the sections were deparaffinized, washed in PBS and H&E staining was performed by standard method. For immunohistochemistry, antigen retrieval was done using Na-citrate buffer (pH-8.5) for 30 seconds. The slides were then incubated for 1 hour in the blocking solution comprising of 3% BSA/PBS. 0.01% Triton X-100 was used to permeabilize the cells for 10 minutes. This was followed by incubation in primary antibody (1:250 dilutions) for 24 hours at 4°C. The following primary antibodies were used in the experiment: GATA-4, A2B5, Brachyury, Insulin, β-III tubulin and Desmin (all from Chemicon). The slides were then washed thrice with PBS; FITC/Alexa Fluor 594-labeled secondary antibodies were added at 1:500 dilutions and incubated for 2 hours. DAPI (Sigma) was used for nuclear staining followed by a final wash with PBS. Negative controls were done without primary antibodies. Slides were mounted with DABCC (Sigma) and images were acquired using NIKON ECLIPSE 90i Microscope (Nikon Corporation) and Image Pro Express Software (Media Cybernetics, Inc., MD, USA).

Flow Cytometry. The hEBs grown on matrigel coated plates were collected by trypsinization at days 8, 14, 21 and 28 for analyses of lineage compositions. The cells were processed for fixation, permeabilization, antibody incubation and analysis as per procedures described in our previous publications. Percentage of differentiated cells in the samples were determined using a set of lineage specific markers including Nestin, Neurofilament heavy chain (NFH), Brachyury, Ventricular myosin, Cytokeratin-18 (CK-18) and Albumin (all from Chemicon).

Estimating Secreted Levels of Proteins by Biochemical Assays. The culture supernatants (spent media) collected at different time points during differentiation were tested for estimation of protein secretion associated with the formation of functional ecto-, meso- and endoderm. We examined the presence of intact ProBNP II, Dopamine, Troponin-T, AFP, Albumin and hCG+β subunit. The analyses of AFP and hCG were done using electrochemiluminescence immunoassay (ECLIA) for these molecules with Roche Elecsys Cobas diagnostic kits (Catalog numbers: 03271749 and 04481798). For albumin, the method employed uses bromocresol green as the anionic dye for binding with albumin which has been standardized against the reference preparation; this was done on Roche/Hitachi Cobas-C system. The method for ProBNP II has been standardized against the Elecsys proBNP assay (Cat. No. 03121640) and the reference method used was Gravimetry. For Troponin-T, calset 04856627 (fur RP

TnT 4.Gen 04491815) was used for calibration which is traceable to In-house reference system, and the concentration of calibrators were 0.0078 and 10.1 ng/ml, respectively. The assays were carried out in triplicates, following the manufacturer's instructions, and were analyzed on the Roche Elecsys 2010 (Roche Diagnostics) immunoassay analyzer. Quantification of dopamine secretion was done by HPLC method (Shimadzu) and the analysis was carried out using LC-MS/MS (Varian) followed by recovery studies.

Statistical Analysis. Data are presented as mean ± SEM. Results were analyzed by one-way ANOVA with Tukey's multiple comparison post test for more than two groups. Differences were considered statistically significant when $P < 0.05$.

Results

It is worth mentioning that we have performed three independent differentiation experiments including once at our new stem cell facility in Malaysia by separate researchers as a third party validation. To our expectation, we were able to exactly reproduce the data from early to late passages of HUES-9 and HUES-7 (28 & 18, 35 & 37, 51 & 54, respectively). Hence the results shown and discussed in this manuscript are all inclusive data from three replicates.

Expression of Pluripotency Markers and Cytogenetic Stability in HUES-9 and HUES-7 Cell Lines. Although these hESC lines are widely used and have demonstrated over time their self-renewal capacity separately by many independent investigators, it was imperative that we re-confirm their pluripotent characteristics at late passages (Fig. 1A & E). We examined the expression of pluripotency markers in HUES-9 and HUES-7 both at mRNA and protein levels at passage 51 and passage 54, respectively. Immunostaining analysis demonstrated that individual hESC lines were similar with respect to expression of Oct-4 and E-cadherin (Fig. 1C, D & G, H). However intensities of the expression of pluripotent genes such as Oct-4, Nanog and ABCG2 in the hESC lines using real-time PCR were different. RNA from two different batches of these lines showed consistently that the levels of Oct-4, Nanog and ABCG2 in HUES-7 was slightly higher than HUES-9 (Fig. 1I). Upon cytogenetic analysis, HUES-9 (46, XX) showed an inversion on chromosome 9 while HUES-7 (46, XY) showed a normal karyotype at passages 51 and 54, respectively (data not shown). Similar karyotype results were obtained in the differentiated cells generated from both cell lines at the other early and late passages mentioned earlier. This demonstrated that the hES cells retained their genetic stability throughout the study.

Comparative Analysis of Early Developmental Competence During EB Formation. During normal development the embryonic germ layers become apparent in a series of steps referred to as gastrulation, which gives rise to the highly organized fetus. Similarly hESCs aggregate into three-dimensional structures called embryoid body (EB) when cultured in suspension consisting of all three embryonic germ layers as well as extraembryonic tissues. The EBs were formed from both the cell lines when they were plated onto non-adherent bacteriological petri dishes and allowed to differentiate for 8 days without bFGF. We did not observe any significant difference in the efficiency of EB formation in terms of pattern and morphology between these cell lines as evident by bright field microscopy (Fig. 1B & F).

The overall incidence of lineage-specific differentiation was evaluated by immunostaining and flow cytometry analysis of EBs which illustrated that all three embryonic germ layers including primitive endoderm were efficiently generated in each case; however, the lineage-specificity during spontaneous differentiation differed among the hESC lines. The EBs generated from HUES-9 and HUES-7 contained many cells that expressed Nestin (Fig. 2A1–A3 & A4–A6) and Keratin 3/12 (K3/K12) (Fig. 2A7–A12), both of which are indicative of neuroectodermal differentiation (21). Further FACS analysis revealed that HUES-7 had relatively higher nestin-positive population (54% ± 7.42) as compared to HUES-9 (49% ± 6.40) (Fig. 2A13, A15 & Table 1). On the contrary expression of NFH, which is a major axonal cytoskeleton protein, was higher in HUES-9 (65.7% ± 1.72) than HUES-7 (41.5% ± 4.33) (Fig. 2A14, A16 & Table 1). Notably formation of neural rosettes and sprouting of neural processes were more frequent in the HUES-9-derived EBs starting from day 4 in differentiation cultures (Fig. 5A, C).

We checked for mesoderm differentiation by the expression of Brachyury (Fig. 2B1–B3 & B4–B6), a T-box transcription factor responsible for development of mesoderm (22) and MyoD which is another putative marker linked to myogenic differentiation (23). The HUES-7-derived EBs contained a larger number of cells expressing Brachyury (74% ± 6.97), whereas such cells were relatively less in the EBs derived from HUES-9 (28.3% ± 4.23) (Fig. 2B13, B15 & Table 1). Further the distribution of MyoD protein in the EBs demonstrated a somewhat uniform pattern in both cell lines (Fig. 2B7–B9 & B10–B12). However, to our surprise, the expression of ventricular myosin, a constituent protein associated with the contraction of ventricular cells in the heart, was found to be slightly higher in HUES-9-derived EBs by flow cytometry (17.5% ± 1.75) in contrast to HUES-7 EBs (3.29% ± 1.87) (Fig. 2B14, B16 & Table 1).

In embryogenesis α-fetoprotein (AFP), Cytokeratin 18 (CK-18) and Albumin are hepatic markers associated with early and late stages of liver development (24). Immunostaining demonstrated that, although HUES-9- and HUES-7-derived EBs steadily expressed AFP (Fig. 2C1–C3 & C4–6) and Albumin antibodies (Fig. 2C7–C9 & C10–C12), the distribution of Albumin was rather spotty in HUES-9. FACS analysis showed that EBs derived from HUES-9 and HUES-7 contained a fairly large percentage of CK-18

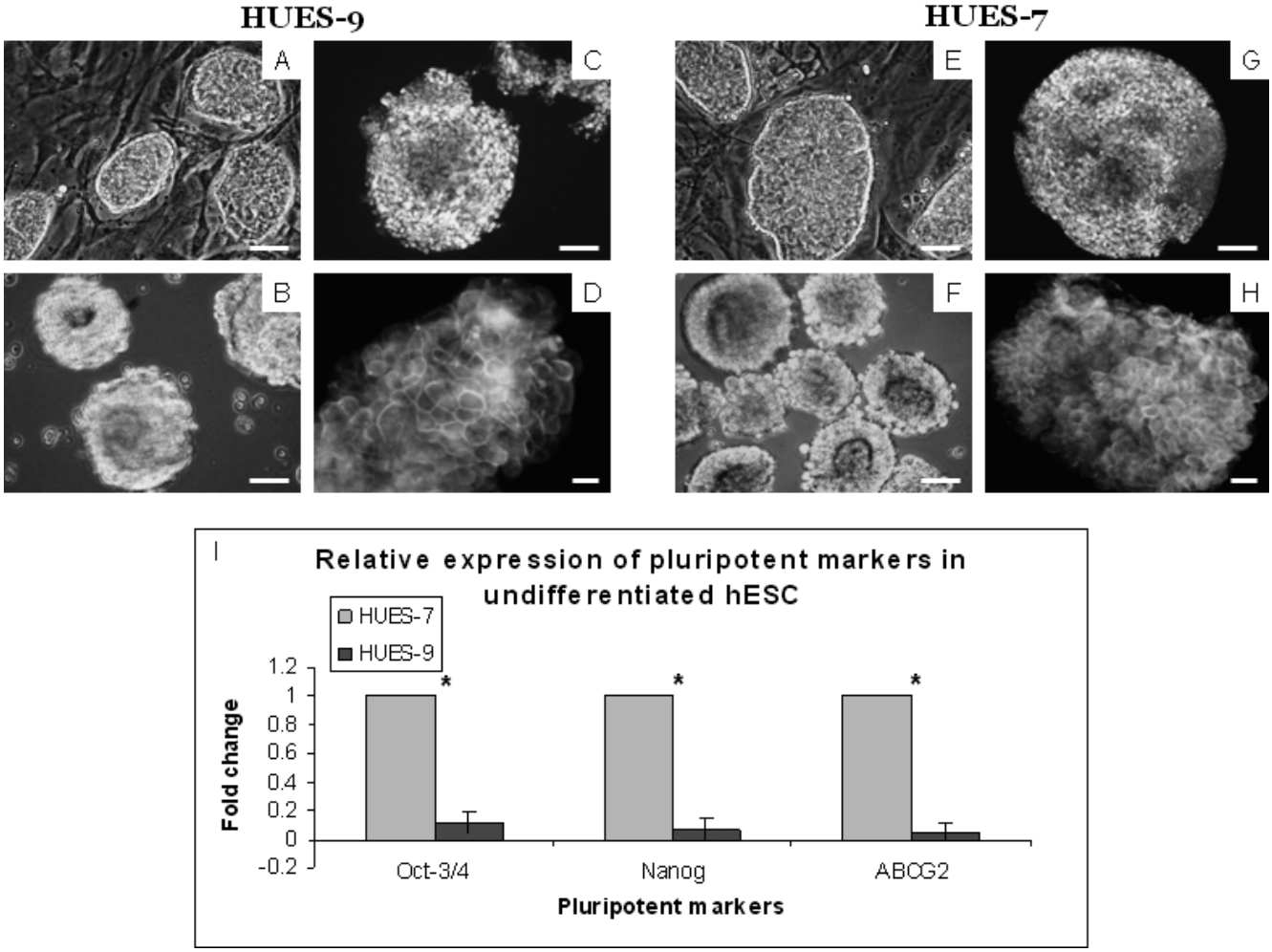

Figure 1. Test of pluripotency in two hESC lines. (A) and (E) showing phase contrast images of day 4 hES colonies of HUES-9 and HUES-7 cell lines grown on MEF, respectively; (B) and (F) demonstrates that both cell lines can be efficiently induced for EB formation in suspension cultures; (C, D) and (G, H) immunostaining for pluripotency marker Oct-4 and adherence junction marker E-cadherin in HUES-9 and HUES-7 colonies. Bars: 50–100 μm. (I) Real-time Q-PCR analysis showing the expression of pluripotency and self-renewal genes, Oct-4, Nanog and ABCG2; although all markers were present in both the cell lines, a small difference in their relative levels was detected. Fold change was determined by using the ΔΔCt method and expression of each gene was normalized to the corresponding level of 18S rRNA gene. Statistically significant changes (* $P < 0.05$) were determined by comparing to HUES-7. Data in the graph is given as mean ± SEM with 3 independent experimental runs, with 3 replicates taken in each run. A color version of this figure is available in the online journal.

positive cells (39% ± 3.77 and 42% ± 2.35, respectively); whereas albumin immunoreactivity was significantly higher in HUES-7 (58% ± 1.73) as compared to HUES-9 (13% ± 2.22) (Fig. 2C13, C15 & Table 1). Enhanced expression of Albumin in HUES-7 directly co-related with the higher number of polygonal bi-nucleated epithelial-like cells after 14–18 days in differentiation which is typical of hepatocytes (Fig. 5I).

Assessment of Gene Expression Associated with the Formation of Three Germ Layers. The divergence in early commitment between the two different hESC lines was confirmed by gene expression analysis. In addition to the markers used in immunostaining and flow cytometry, several genes were analyzed by RT-PCR. Nestin and β-III tubulin are putative markers to be expressed in neuroectodermal cells and also in neuronal progenitors. In consensus with the results obtained by immunostaining and FACS, neuroectodermal markers including Nestin and β-III tubulin were expressed in HUES-9- and HUES-7-derived EBs (Fig. 3A, B). However, both these genes were feebly upregulated in HUES-9 compared to HUES-7 (Fig. 3A).

A number of genes are known to be expressed exclusively in the mesendoderm. Likewise, heart and neural crest derivatives expressed 1 (HAND1); GATA binding proteins 2 and 4 to be expressed in definitive endoderm and cardiac mesoderm; hepatocyte nuclear factor 4 (HNF-4), a variant form of HNF-1 (also called HNF-1β) is associated with early endoderm development (25); endoderm-derived growth factor from TGF-β superfamily member, bone morphogenetic protein 4 (BMP-4) and Brachyury were used to show the formation of mesoderm and endoderm. HAND1, GATA-4, HNF-4 and Brachyury showed consis-

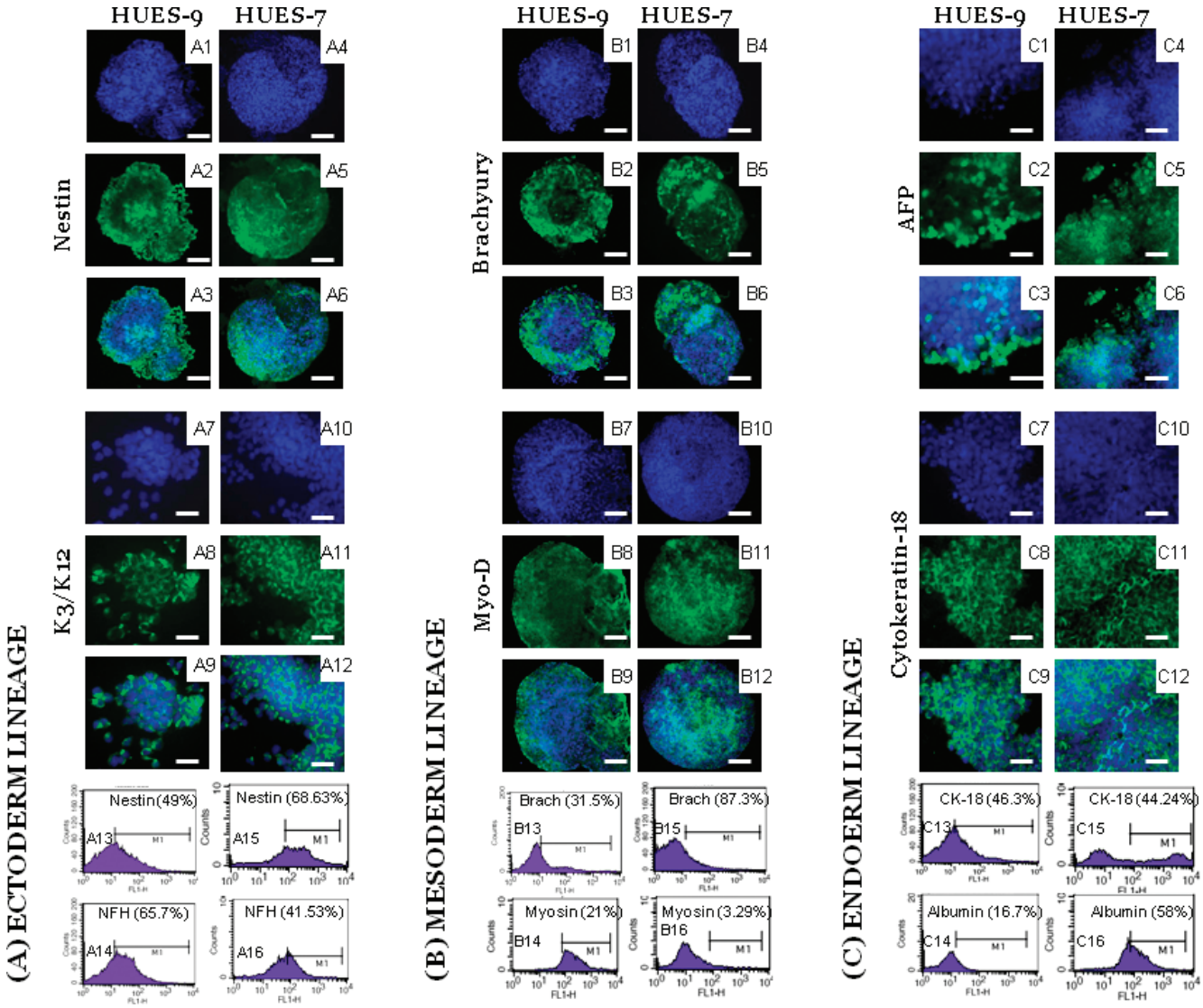

Figure 2. Comparing the differentiation potential of the hESC lines into (A) ectoderm, (B) mesoderm and (C) endoderm lineages. (A1–A6) Representative immunofluorescence images of HUES-9- and HUES-7-derived day 8 EBs stained for early stage neural marker Nestin; (A7–A12) limbal epithelial marker K3/K12; (B1–B6) early mesoderm marker Brachyury; (B7–B12) myogenic differentiation marker MyoD; (C1–C6) fetal liver marker AFP; (C7–C12) hepatocyte differentiation marker CK-18. FITC was used as the conjugate and DAPI as counter stain; bars: 100 μm. (A13–A16) Histograms obtained by FACS analysis showing difference in HUES-9 and HUES-7 lines towards neuroectoderm induction using Nestin and NFH antibodies; (B13–B16) mesoderm induction using Brachyury and MyoD antibodies; (C13–C16) endoderm induction using CK-18 and Albumin antibodies. Appropriate isotype controls were used to gate the positively stained sub-population.

tent expression in the EBs generated from HUES-9 and HUES-7 (Fig. 5A, B). Although the level of GATA-4 expression in EBs derived from HUES-7 was higher than in the HUES-9, this does not necessarily imply that the former EBs contain a higher proportion of endoderm cells because GATA-4 also shows transitory expression in the mesoderm (26).

Human chorionic gonadotrophin β subunit (HCG-β) and CDX-2 genes are expressed at different stages of primordial germ cell development in both males and females, and are hence used as markers for trophectoderm in hESCs (27). The two hESC lines showed very low or no detectable levels of CDX-2 expression, but expression of HCG-β was variable and was in fact higher in HUES-9- than HUES-7-derived EBs (Fig. 3A, B). Taken together, these results indicate that both the cell lines are capable of generating germ cells but that the degrees of their formation vary to some extent.

Morphology and Structural Characteristics of EBs Impact Their Spatio-Temporal Differentiation into Putative Germ Layers. Even while maintenance, hESC cultures fail to represent a purely homogeneous pluripotent population but randomly show-up hESC-derived differentiated cells (28). Therefore the composition of the input hESC population varies between passages and could influence cell fate trajectory during early differentiation.

Table 1. Flow Cytometry Analysis of Differentiated Cells Using Lineage and Tissue Specific Protein Markers

		HUES-7			HUES-9		
Name of the marker	Passage[a]	% positive cells	Mean	SEM	% positive cells	Mean	SEM
Nestin	Late	49	49.00	6.404	68.63	54	7.423
	Middle	55			63.5		
	Early	61.8			54		
NFH	Late	65.7	65.7	1.724	41.53	41.53	4.336
	Middle	69.1			50.2		
	Early	67.9			46		
Brachyury	Late	31.5	28.3	4.239	87.3	74	6.975
	Middle	28.3			74		
	Early	36.7			77		
Ventricular myosin	Late	21	17.5	1.756	3.29	3.29	1.877
	Middle	17.5			6.9		
	Early	19			4.2		
CK-18	Late	46.3	39.00	3.772	44.2	42	2.351
	Middle	41			46.7		
	Early	39			42		
Albumin	Late	16.7	13	2.228	58	58	1.732
	Middle	17			61		
	Early	13			58		

[a] Late passage: P51 (HUES-9) & P54 (HUES-7); middle passage: P35 (HUES-9) & P37 (HUES-7); and early passage: P28 (HUES-9) & P18 (HUES-7).

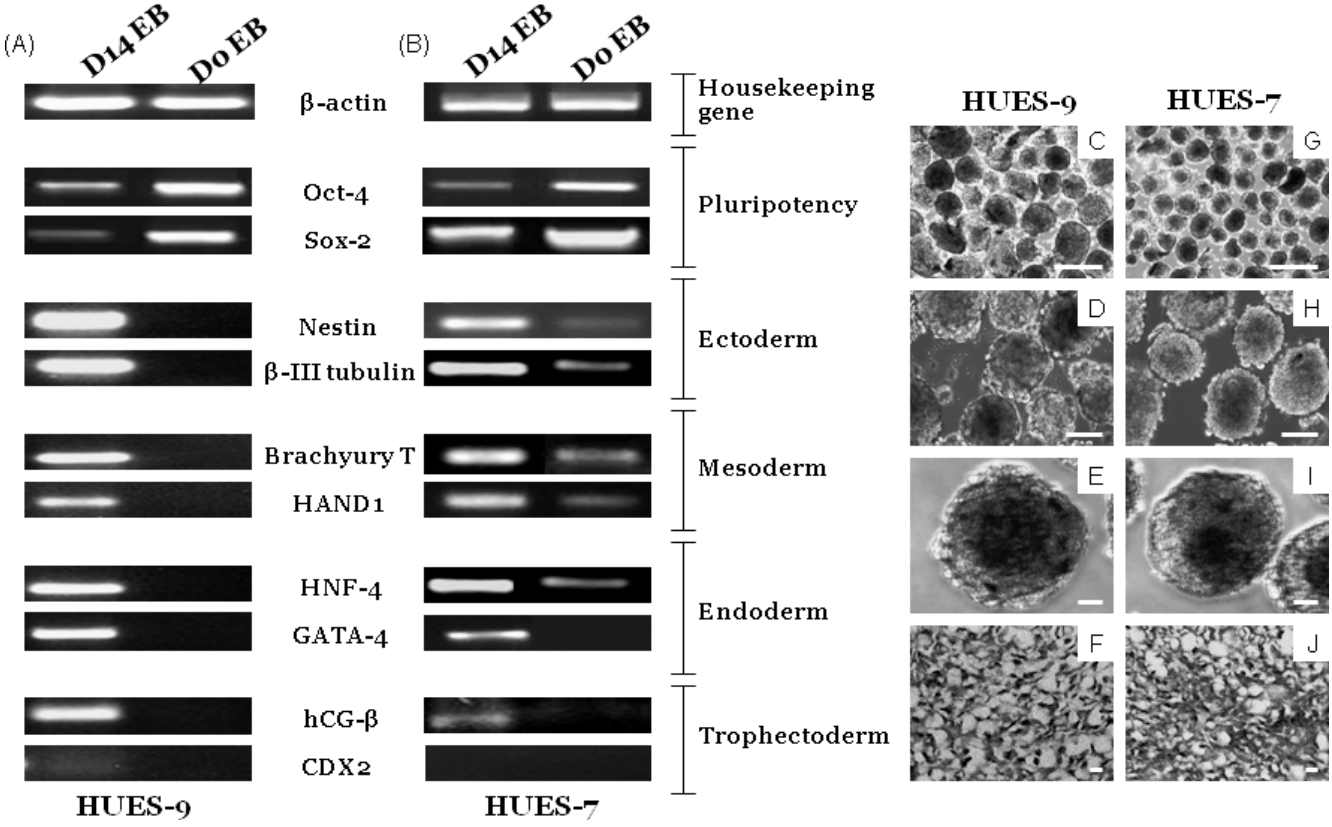

Figure 3. Gene expression profile associated with the formation of three germ layers. (A) and (B) Representative RT-PCR analysis for genes specific for embryonic germ layers such as ectoderm, mesoderm, endoderm, including trophectoderm; all the genes, although activated in both cell lines HUES-9 and HUES-7, display minor variations in their expression pattern. We induced EB formation in large-scale employing trypsinization method as mentioned earlier. (C) and (G) shows phase contrast images of HUES-9- and HUES-7-derived day 8 EBs in mixed shapes and sizes; (D) and (H) EBs selected manually under stereomicroscope based on their size and morphology; (E) and (I) isolated matured EB with distinct "blood islets" under higher magnification. (F) and (J) H&E staining demonstrating the histology of paraffin-embedded EB sections revealed that the aggregates are non-cystic and thereby free of apoptotic cells as witnessed in case of both cell lines; bars: 50–300 μm.

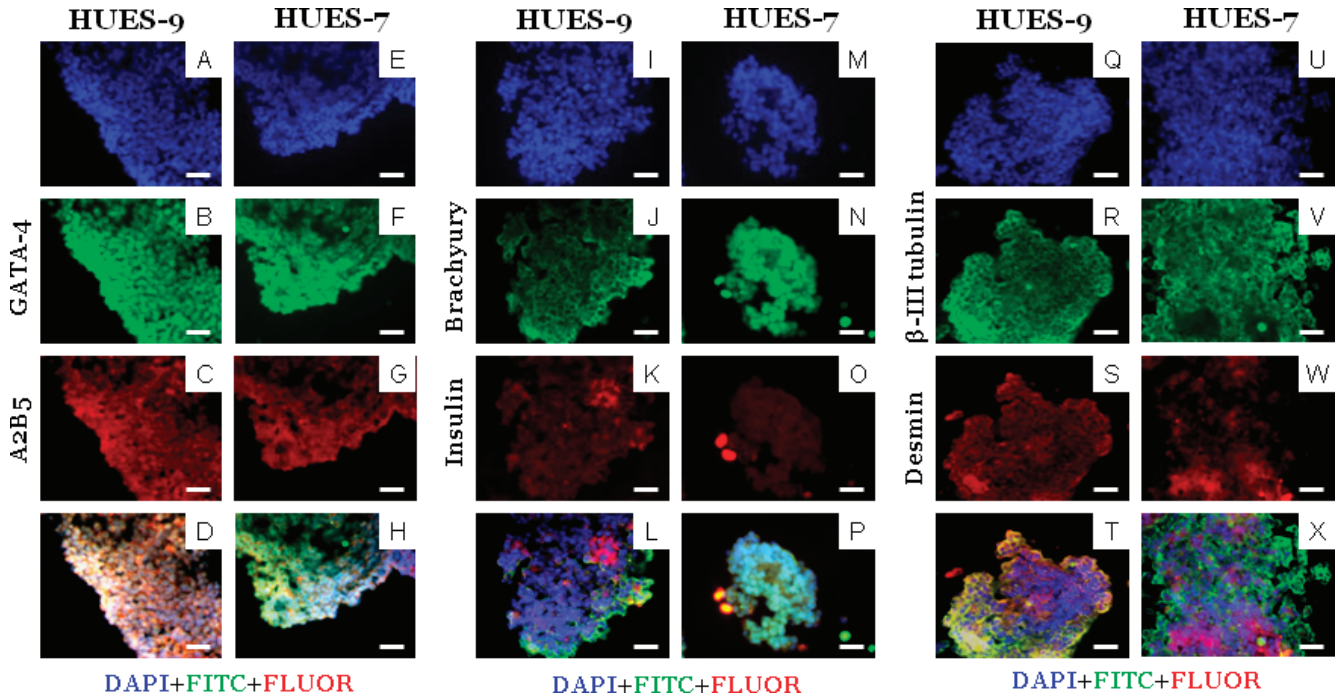

Figure 4. Distribution of lineage and tissue specific markers in three-dimensional EBs. Representative immunofluorescence images of paraffin-embedded EB sections stained for combination of several markers to emphasize that the cells are capable to generate all three germ layer derivatives at one time (A–D, E–H, GATA-4/A2B5), (I–L, M–P, Brachyury/Insulin) and (Q–T, U–X, β-III tubulin/Desmin). Although the proteins co-expressed in EBs derived from HUES-9 and HUES-7, a slender difference was noticed in the distribution pattern of Insulin and Desmin; further neuroectoderm markers like A2B5 and β-III tubulin were localized more towards the periphery whereas mesendoderm markers were abundant in the central regions of the EBs. Here FITC and Alexa Fluor-594 were used as the two conjugates and DAPI as the counter stain; bars: 100 μm.

Colony size is also a critical parameter in determining self-renewal and differentiation outcome as hESCs depend on paracrine signals from adjoining undifferentiated cells to antagonize pro-differentiation signaling pathways (17). Lastly, EB size and morphology could affect differentiation outcome as modulation of this parameter may trigger spatial signaling within these aggregates.

Similar to mouse, human EBs grown for 7–8 days often display central cavities indicative of cavitation (29). Subsequent culture up to 10 days or more yields morphologically heterogeneous EBs containing fluid-filled cysts, termed cystic EBs. Further it has been demonstrated that extensive apoptosis takes place during cavitation of EBs which might perturb their capacity of subsequent expansion and differentiation (30). Because of their heterogeneity, our study was designed to focus on the characterization of differentiation events within normal EBs for improved reproducibility. In our study we performed enzymatic dissociation of hESCs in place of hanging drop method in order to support our efforts towards large scale EB production. Owing to this, we found that the individual EBs thus formed displayed non-uniform morphological characteristics and thereby represented dissimilar stages of hESC differentiation (Fig. 3C & G). Therefore, we opted for manual sorting of EBs which showed uniform morphological features such as round shape, compactness and medium size (Fig. 3D & H). Thereafter both HUES-9- and HUES-7-derived EBs displayed comparable morphology with the presence of "blood islets" as revealed by phase contrast microcopy (Fig. 3E & I). Additionally histological studies by H&E staining of the EB sections have shown that these aggregates are devoid of any cavities, which is why they demonstrate non-cystic morphology and such compactness (Fig. 3E, F & I, J).

Passages 51–54 hESCs were mechanically dissected, grown in suspension for 4 to 8 days harvested and processed; paraffin embedded sections were prepared and then immunohistochemical (tri-color, DAPI/FITC/Alexa Fluor) staining was performed with a panel of specific antibodies. The scheme was such that the co-expression of three possible combinations of markers associated with the formation of all germ layers, namely ecto-endo (A2B5/GATA-4), meso-endo (Brachyury/Insulin) and ecto-meso (β-III tubulin/Desmin), could be effectively analyzed. For all markers tested, results are representative of at least 10 EBs observed at each time point. Prior to suspension culture, hESCs exhibited Oct-4 immunoreactivity but failed to show detectable immunoreactivity to A2B5, β-III tubulin, Brachyury, Desmin, GATA-4 and Insulin. Following 3–4 days in suspension culture spheroid aggregates of different sizes and shapes were formed from both the cell lines HUES-9 and HUES-7 (Fig. 3C & G). However, in order to eliminate predisposition due to variation in EB size leading to any favoritism in lineage specification, we selected only

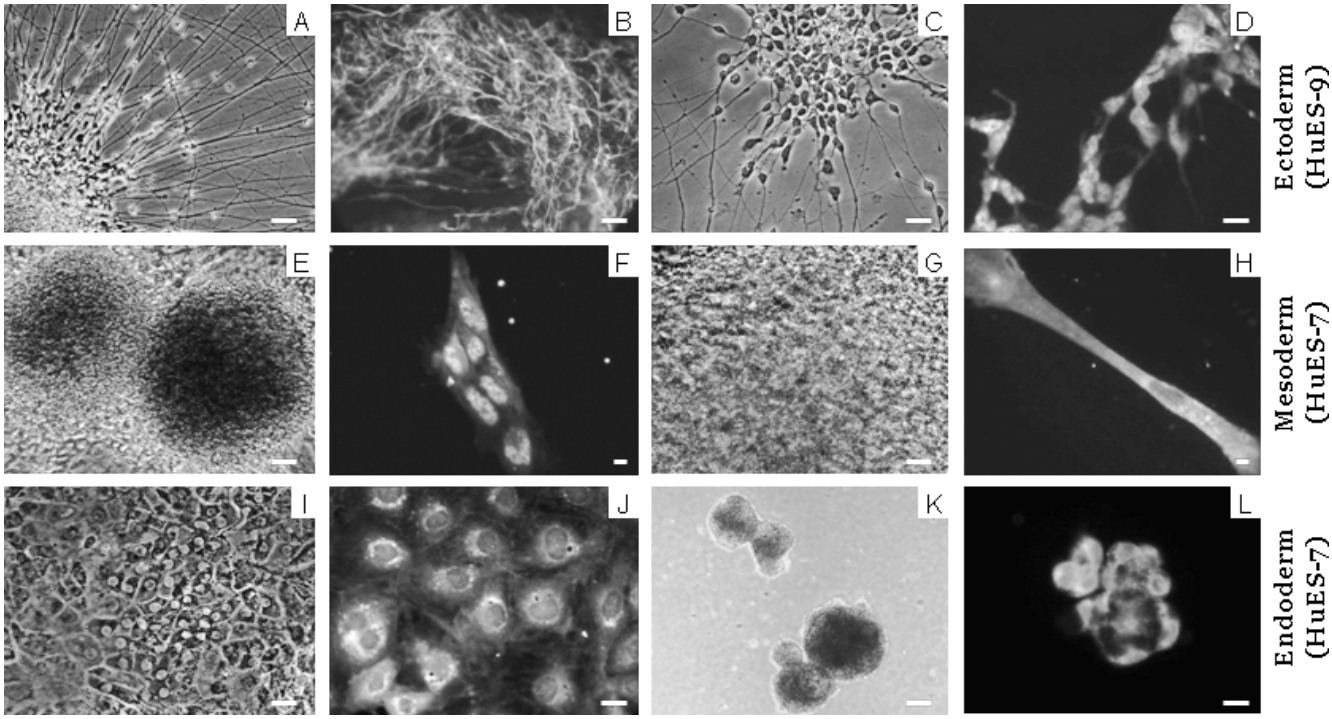

Figure 5. Development of EBs into mature cell types. Phase contrast image of differentiated cells including (A) neurons, (C) astrocytes and oligodendrocytes, (E) flat cardiac bodies, (G) beating cardiomyocytes, (I) hepatocyte-like cells and (K) pancreatic bud-like structures that migrated out of HUES-9- and HUES-7-derived EBs. Likewise, immunofluorescence images of HUES-9-derived cells stained for markers of motoneurons and interneurons (B, D, β-III tubulin and A2B5, respectively); (F, H, Brachyury and Ventricular myosin heavy chain-β) which are cardiac precursor and mature cardiomyocyte markers, respectively; (J, L, Albumin and Insulin) associated with hepatocytes and pancreatic β-islets, respectively. We used FITC as the conjugate; bars: 100 μm.

the round and compact EBs under the stereomicroscope and allowed them to grow further up to day 8. At this time point A2B5 and GATA-4 were expressed both centrally and towards the periphery in HUES-9- and HUES-7-derived EB sections (Fig. 4A–D & E–H). Interestingly Brachyury was expressed in cells towards the EB periphery in HUES-9 but was observed within the interior of EBs derived from HUES-7 (Fig. 4J, L & N, P). Immunoreactivity to insulin could only be detected in discrete patches towards the central part of the EBs, predominantly in HUES-9 (Fig. 4K, L & O, P). Furthermore β-III tubulin immunoreactivity broadly appeared all over the EBs, whereas localization of Desmin antibody was rather occasional and restricted to some isolated regions of the HUES-9- and HUES-7-derived EBs (Fig. 4Q–T & U–X).

Evaluation of the Differentiation Capacity of EBs Toward Mature Cell Types. To investigate whether the differences detected in early stages of lineage commitment were preserved during the course of terminal differentiation, day 8 EBs derived from the two hESC lines were plated onto matrigel coated tissue culture dishes and allowed to differentiate into more mature cell types in the same medium without inducing factors. Over 8 days numerous cells of heterogeneous morphology drifted out of the attached EBs. To our expectation, the patterns of differentiation of the individual hESC lines resembled the early developmental potentials witnessed in the EBs. For the first 4 days a large number of bipolar cells forming elongated processes migrated from the HUES-9-derived EBs (Fig. 5A & C). In contrast, the majority of cells that emerged from HUES-7-derived EBs had a flat epithelial morphology and comparatively fewer cells had the appearance of neural precursors or putative neurons. After 8 days in differentiation, immunostaining revealed that the majority of bipolar cells and the sprouting neural processes of HUES-9-derived EBs expressed the neuronal marker β-III tubulin (Fig. 5B) and some of them also expressed A2B5, a marker for astrocytes and gangliosides (Fig. 5D). Upon comparing the overall expression levels of neurogenesis-associated SOX-1 gene, neural differentiation was found to be consistently higher in HUES-9 (58.89 fold ± 12.10) than in HUES-7 (8.69 fold ± 1.18) (Fig. 6A).

We next compared the ability of the two hESC lines to form mesodermal derivatives. As noted previously, many cells migrating out of HUES-7-derived EBs exhibited flat epithelial morphologies; some of these cells eventually aggregated forming single to multi-layered beating cardiac bodies and vascular endothelial networks (Fig. 5E & G). Immunostaining revealed that these mono- and bi-layered cardiac and vascular structures were strongly positive for Brachyury, a mesoderm marker, and Ventricular myosin heavy chain-β, a mature cardiomyocyte marker. Although

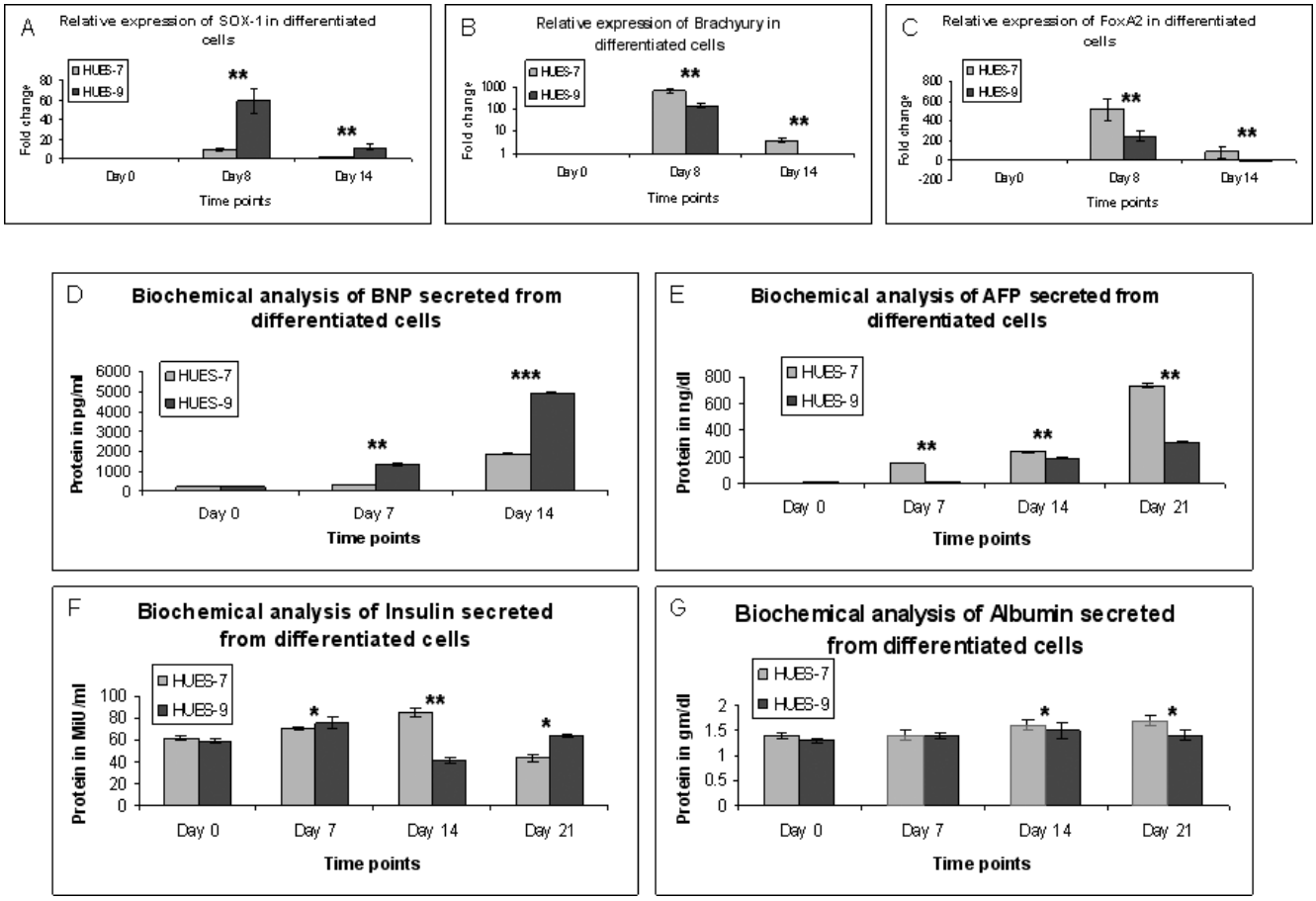

Figure 6. Determination of key mRNA transcript levels and estimation of protein production associated with lineage-specific differentiation. (A–C) Relative levels of expression of neuronal (SOX-1), cardiac (Brachyury-T) and hepatic (FoxA2) genes in the HUES-7- and HUES-9-derived cells from days 0 to 14 as detected by real-time Q-PCR; fold change was calculated employing the ΔΔCt method and expression of each gene was normalized to the corresponding 18S rRNA level. Quantitative biochemical analysis (ECLIA) of (D) BNP (brain), (E) AFP (fetal liver), (F) Albumin (liver) and (G) Insulin (pancreas) protein secreted in spent culture supernatants collected from hESC-derived cells from days 0 to day 21. All data is representative of three separate experiments and was confirmed to be in concordance with the basal levels of corresponding proteins detected in human blood samples. Statistically significant changes (* $P < 0.05$; ** $P < 0.01$; *** $P < 0.001$) were determined by comparing to HUES-7. Data in the graph is given as mean ± SEM with 3 independent experimental runs, with 3 replicates taken in each run. A color version of this figure is available in the online journal.

Brachyury was abundantly found in these cultures, Ventricular myosin heavy chain-β positive cells were rarely detected (Fig. 5F & H). The preferential differentiation into mesodermal derivatives of HUES-7 was further corroborated by real-time PCR analysis of Brachyury-T which was much highly expressed in HUES-7 (714 fold ± 169.41) compared to HUES-9 (156 fold ± 34.96) (Fig. 6B).

Likewise endodermal derivatives mainly definitive and gut endoderm-like cells dominated the HUES-7 cultures as clusters or discrete patches from days 4–6 onwards. At day 8, large patches of cells from HUES-7-derived EBs gave rise to cells which were polygonal in morphology and occasionally contained double nuclei, features typical of mature hepatocytes (Fig. 5I); whereas EBs grown in suspension for more than 10 days from both HUES-9 and HUES-7 started giving out pancreatic bud-like outgrowths (Fig. 5K). Nevertheless, the most frequently observed endodermal cell type was the hepatocyte. As in normal liver development, Albumin, a very well-known hepatocyte marker, was expressed in majority of these epithelial-like cells (Fig. 5J) predominantly in HUES-7 cultures. These cultures also showed positive expression for Insulin, a key marker of pancreatic-islet differentiation, more often in the cells comprising the clusters and the protruding bud-like structures (Fig. 5L). Comparative analysis of early endoderm-associated gene expression confirmed the results of immunostaining showing that FoxA2 was not only upregulated (512 fold ± 108.76) but also retained its strong presence during terminal differentiation of HUES-7 (245.57 fold ± 45.90) than in HUES-9 (–10.33 fold ± 2.62) (Fig. 6C).

Then, we selected a subset of early lineage as well as tissue specific proteins associated with the development and maintenance of neuroectoderm and definitive/gut endoderm and estimated their levels of secretion in the spent medium at progressive days of EB differentiation. We found that the

levels of BNP was much higher at day 14 (1365 pg/ml ± 56.74) through day 21 (4945 pg/ml ± 34.01) in HUES-9 compared to HUES-7 (Fig. 6D). In contrast, the secreted levels of AFP, Albumin and Insulin at day 21 (734 ng/dl ± 14.65; 1.7 gm/dl ± 0.01 and 85.48 MiU/ml ± 3.59, respectively) in HUES-7 was significantly higher than in HUES-9 (Fig. 6E–G). Notably, for all these assays developed we used undifferentiated hESC as the internal control and have also considered the basal levels of these molecules in an adult human male as reference standards. Although we also performed quantitative analysis of dopamine and cardiac troponin-T proteins, the results obtained were not statistically significant and hence not included in this manuscript (data not shown).

Discussion

Presently hESCs are considered as an excellent in vitro model to understand the intricacies of early human development as well as for regenerative medicine. However, hESCs hold remarkable potentials in latent applications such as drug screening and toxicity testing that are more apt and instant. Development of improved research tools with better precision using hES cell technology will eventually lead to greater patient safety and also significantly decrease the number of laboratory animals needed for toxicological and pharmacological testing. While hESC lines are continuously being established across the world, relatively fewer studies focusing on the properties of different hESC lines have been conducted so far. Moreover those few studies concentrated mainly on the undifferentiated state, rate of proliferation, cytogenetic and epigenetic stability rather than dealing with the differences in developmental competence in vitro (12, 13, 17, 31–35). Recently Osafune *et al.* (2008) reported marked differences in propensity among 17 hESC lines; notably this study also included HUES-9 and HUES-7 cell lines (36). Furthermore, most of these studies employed transcription profiling as an index to predict variation among the cell lines which leaves behind a scope for further investigation at protein production and enzyme activity studies.

In contrast to human embryonal carcinoma cells such as the NTERA-2 cell line, which shares similar properties with hESC in terms of pluripotent marker expression (37, 38), undifferentiated hES cells have strong inclination for spontaneous differentiation to various cell types. However, too little is known about the complex mechanisms that govern spontaneous differentiation of pluripotent hESC into a heterogeneous population of early progenies. Spontaneous differentiation of hESC despite redundant and anecdotal is inevitable to certain extent in most routine cultures (39). However efforts are ongoing to devise better strategies to get rid of spontaneous differentiation which offers a major challenge in hESC maintenance and scale-up (40). On the other hand this phenomenon of spontaneous differentiation in hESC can be harnessed to study early embryonic development by recapitulating certain aspects of the process. This understanding may provide guidelines in designing better differentiation protocols either based on the propensity of the cell line towards a specific lineage or by modulating the time, duration and stage of differentiation induction. Ultimately it might lead to successful generation of a variety of hESC derivatives in large numbers for stem cell transplantation and drug screening programs.

The aim of the present study was to acquire a thorough understanding of the potential diversity in differentiation penchant that exists among two hESC lines, HUES-9 and HUES-7. We anticipated that the biological differences among hESC lines could have a considerable impact on their propensity during spontaneous differentiation. We first examined spontaneous differentiation via EB formation without added growth factors to minimize any partiality in differentiation. In three independent experiments samples were taken at four time points: the start of EB formation (undifferentiated hES cells; day 0) and EBs at culture days 8, 14 and 21. Expression and production levels of total 26 marker genes and proteins representative of the undifferentiated state, the three germ layers and six derivative organs were assessed by semi-quantitative RT-PCR, quantitative RT-PCR, immunocytochemistry, immunohistochemistry, flow cytometry, histopathology and ECLIA. Our data clearly suggest that individual hESC lines follow different developmental trajectories although they show similar pattern of marker expression at the undifferentiated state.

Both the cell lines HUES-9 and HUES-7 efficiently generated the three germ layers, extraembryonic tissues and primordial germ cells during EB formation. However, the proportions of each germ layer or other embryonic cell types in the EBs varied depending on the developmental competence of the cell line. HUES-9 readily formed neuroectodermal lineage, whereas HUES-7 preferentially differentiated into mesodermal and endodermal lineages. This was obvious from the results obtained by RT-PCR wherein the expression levels of Nestin and β-III tubulin was significantly higher in HUES-9 compared to HUES-7. The trend was similar in case of SOX-1 gene as detected by Q-PCR; furthermore it was observed that SOX-1 expression was retained up to differentiation day 14 unlike in HUES-7. This finding suggests that the initial induction towards neuroectoderm lineage is stronger in the case of HUES-9-derived EBs which resulted in further differentiation and enrichment of neural cells, thereby presenting enhanced expression of mature markers including NFH and BNP. Nevertheless the high percentage of nestin-positive cells in HUES-7, despite having a lower propensity towards neuroectoderm lineage than HUES-9, may be attributed to the transient expression of nestin in embryonic insulin-producing pancreatic-islets (41). Moreover the neural fate is regarded as the default pathway of mouse ESCs (42); so hESCs adopting a similar route of differentiation was not surprising. Moreover transcriptional profiling of ESCs and

neural stem cells (NSCs) revealed that both these type of stem cells are similar in their overall blueprint of gene expression patterns endorsing the idea of a neural default pathway (43). Our data clearly indicates that HUES-9 consistently follows this default pathway whereas HUES-7 does not. The neural default pathway depends on inhibition of bone morphogenetic protein (BMP) signaling by antagonists such as noggin, chordin, cerberus and follistatin (44). So one possible explanation may be the inhibition of BMP signaling is inefficient in HUES-7; this was further concurrent with our data showing an upregulation of BMP-2 and BMP-4 genes (data not shown). Notably, we also tested the capacity of HUES-9 to give rise to limbal epithelial cells, another important component of the neuroectoderm lineage by demonstrating immunoreactivity to K3/K12 antibody (Fig. 2A7-A12).

Likewise HUES-7 generated a higher percentage of mesoderm and endoderm cells than HUES-9. The parallel increase in mesoderm and endoderm was not unexpected given that these two germ layers are known to originate from a common precursor mesendoderm (45). In our study we detected a higher proportion of cells immunoreactive towards Brachyury, CK-18 and Albumin. This was further confirmed by activation of Brachyury and FoxA2 genes by Q-PCR followed by an enhanced production of AFP, Albumin and Insulin proteins by ECLIA. The co-expression of heart and liver markers in HUES-7-derived EBs is in accordance with the hypothesis that during ESC differentiation there is an existing obligatory interaction among the cardiomyocytes and hepatocytes in vitro (46) which further conforms to the experimental results conducted in animal models (47). It has also been reported that nodal, a member of the transforming growth factor-beta (TGF-β) superfamily, enhances the development of mesendoderm in mouse embryos (48) and inhibits differentiation along the neuroectodermal default pathway in hESCs (49). This phenomenon is similar to what was witnessed in HUES-7 as it barely forms functional neurons. Despite having an inclination to mesendoderm formation, HUES-7 did not readily activate pancreatic genes except sporadic expression of insulin protein.

Although the experiments described in this study do not elucidate the specific reasons of the variation in differentiation propensity among HUES lines, this data strongly indicates that particular hESC lines may have obtained intrinsic properties that predispose them to possess different in vitro differentiation potential. The variation in propensities between hESC lines during spontaneous differentiation may be the consequence of the conditions and developmental stage under which they were isolated, gender differences, genetic variations, methods of passaging, culture conditions or other unknown factors. Because each hESC line has an exclusive human genome, it is unlikely that all hESC lines would display identical gene expression profiles. Abeyta *et al*. (2004) suggested that single nucleotide polymorphisms (SNPs) contribute to the distinctive expression signatures of individual hESC lines. Epigenetic changes may also affect gene expression patterns as hESC lines possess unique epigenetic signatures (8). This was verified by a study which showed that the extent of DNA methylation of the Oct-4 promoter region can result in different gene expression profiles in hESC lines (9). Recently micro-RNAs (miRNA-302) have been implicated in regulation of pluripotent genes Oct-4, Nanog and Sox-2 thereby modulating ESC differentiation (50). In addition, hESC lines exhibit distinct patterns of X-chromosome inactivation which may influence their developmental competence (10). In our experiments, among the two cell lines, HUES-9 was female and HUES-7 was male. Nevertheless we cannot rule out the possibility of influencing the differences in propensities by the chromosome abnormalities since HUES-9 showed inversion in chromosome 9 (36). Furthermore it is imprudent to judge that female cell lines possess a natural tendency to develop neurons since previous studies have shown that even the male hESC lines including H1, BG01 and BG02 generated neuroectodermal lineages quite efficiently (51–53). One important possibility is that these differences reflect the fact that hESC lines unlike their mouse counterparts are isolated from an outbred population with considerable genetic variation.

In summary, we have shown compelling evidence demonstrating that specific hESC lines have a propensity to produce certain lineages or cell types when allowed to differentiate spontaneously. Our results offer a valuable platform for selecting hESC lines to generate distinct cell types in large numbers and imply that even induced pluripotent stem cells (iPS) might as well show a similar variability. These findings once more draw our attention to the magnitude of deriving additional stem cell lines for specific lineages in clinical research and drug screening purposes. Therefore it emerges that some hESC lines are better suited for a particular application than others and hence researchers should be able to opt for appropriate cell lines for specific applications.

We acknowledge Abexome, Bangalore for providing AFP antibody as a kind gift.

1. Thompson JA, Itskovitz-Eldor J, Shapiro SS, Waknitz MA, Swiergiel JJ, Marshall VS, Jones JM. Embryonic stem cell lines derived from human blastocysts. Science 282:1145–1147, 1998.
2. Keller G. Embryonic stem cell differentiation: emergence of a new era in biology and medicine. Genes Dev 19:1129–1155, 2005.
3. Hoffman LM, Carpenter MK. Characterization and culture of human embryonic stem cells. Nat Biotechnol 23(6):699–708, 2005.
4. Pal R, Khanna A. Similar pattern in cardiac differentiation of human embryonic stem cell lines, BG01V and ReliCellhES1, under low serum concentration supplemented with bone morphogenetic protein-2. Differentiation 75:112–122, 2007.
5. Denning C, Allegrucci C, Priddle H, Barbadillo-Munoz MD, Anderson D, Self T, Smith NM, Parkin CT, Young LE. Common culture conditions for maintenance and cardiomyocyte differentiation of the

human embryonic stem cell lines, BG01 and HUES-7. Int J Dev Biol 50:27–37, 2006.
6. Oh SK, Kim HS, Ahn HJ, Seol HW, Kim YY, Park YB, Yoon CJ, Kim DW, Kim SH, Moon SY. Derivation and characterization of new human embryonic stem cell lines: SNUhES1, SNUhES2, and SNUhES3. Stem Cells 23:211–219, 2005.
7. Ward CM, Barrow KM, Stern PL. Significant variations in differentiation properties between independent mouse ES cell lines cultured under defined conditions. Exp Cell Res 293:229–238, 2004.
8. Bibikova M, Chudin E, Wu B, Zhou L, Garcia EW, Liu Y, Shin S, Plaia TW, Auerbach JM, Arking DE, Gonzalez R, Crook J, Davidson B, Schulz TC, Robins A, Khanna A, Sartipy P, Hyllner J, Vanguri P, Savant-Bhonsale S, Smith AK, Chakravarti A, Maitra A, Rao M, Barker DL, Loring JF, Fan JB. Human embryonic stem cells have a unique epigenetic signature. Genome Res 16(9):1075–1083, 2006.
9. Lagarkova MA, Volchkov PY, Lyakisheva AV, Philonenko ES, Kiselev SL. Diverse epigenetic profile of novel human embryonic stem cell lines. Cell Cycle 5:416–420, 2006.
10. Hoffman LM, Hall L, Batten JL, Young H, Pardasani D, Baetge EE, Lawrence J, Carpenter MK. X-inactivation status varies in human embryonic stem cell lines. Stem Cells 23:1468–1478, 2005.
11. Abeyta MJ, Clark AT, Rodriguez RT, Bodnar MS, Pera RA, Firpo MT. Unique gene expression signatures of independently-derived human embryonic stem cell lines. Hum Mol Genet 13:601–608, 2004.
12. Rao RR, Calhoun JD, Qin X, Rekaya R, Clark JK, Stice SL. Comparative transcriptional profiling of two human embryonic stem cell lines. Biotechnol Bioeng 88:273–286, 2004.
13. Skottman H, Stromberg AM, Matilainen E, Inzunza J, Hovatta O, Lahesmaa R. Unique gene expression signature by human embryonic stem cells cultured under serum free conditions correlates with their enhanced and prolonged growth in an undifferentiated stage. Stem Cells 24:151–167, 2005.
14. Kitsberg D. Human embryonic stem cells for tissue engineering. Methods Mol Med 140:33–65, 2007.
15. Pyle AD, Lock LF, Donovan PJ. Neurotrophins mediate human embryonic stem cell survival. Nat Biotechnol 24:344–350, 2006.
16. Schatten G, Smith J, Navara C, Park JH, Pedersen R. Culture of human embryonic stem cells. Nat Methods 2:455–463, 2005.
17. Peerani R, Rao BM, Bauwens C, Yin T, Wood GA, Nagy A Kumacheva E, Zandstra PW. Niche-mediated control of human embryonic stem cell self-renewal and differentiation. EMBO J 26: 4744–4755, 2007.
18. Ng ES, Davis RP, Azzola L, Stanley EG, Elefanty AG. Forced aggregation of defined numbers of human embryonic stem cells into embryoid bodies fosters robust, reproducible hematopoietic differentiation. Blood 106:1601–1603, 2005.
19. Ungrin MD, Joshi C, Nica A, Bauwens C, Zandstra PW. Reproducible, ultra high-throughput formation of multicellular organization from single cell suspension-derived human embryonic stem cell aggregates. PLoS One 3:e1565, 2008.
20. Burridge PW, Anderson D, Priddle H, Barbadillo Munoz MD, Chamberlain S, Allegrucci C, Young LE, Denning C. Improved human embryonic stem cell embryoid body homogeneity and cardiomyocyte differentiation from a novel V-96 plate aggregation system highlights interline variability. Stem Cells 25:929–938, 2007.
21. Chen Z, de Paiva CS, Luo L, Kretzer FL, Pflugfelder SC, Li DQ. Characterization of putative stem cell phenotype in human limbal epithelia. Stem Cells 22(3):355–366, 2004.
22. Wilkinson DG, Bhatt S, Herrmann BG. Expression pattern of the mouse T gene and its role in mesoderm formation. Nature 343:657–659, 1990.
23. Kamochi H, Kurokawa MS, Yoshikawa H, Ueda Y, Masuda C, Takada E, Watanabe K, Sakakibara M, Natuki Y, Kimura K, Beppu M, Aoki H, Suzuki N. Transplantation of myocyte precursors derived from embryonic stem cells transfected with IGFII gene in a mouse model of muscle injury. Transplantation 82:516–526, 2006.
24. Chen Y, Soto-Gutierrez A, Navarro-Alvarez N, Rivas-Carrillo JD, Yamatsuji T, Shirakawa Y, Tanaka N, Basma H, Fox IJ, Kobayashi N. Instant hepatic differentiation of human embryonic stem cells using activin A and a deleted variant of HGF. Cell Transplant 15(10):865–871, 2006.
25. Abe K, Niwa H, Iwase K, Takiguchi M, Mori M, Abe SI, Abe K, Yamamura KI. Endoderm-specific gene expression in embryonic stem cells differentiated to embryoid bodies. Exp Cell Res 229:27–34, 1996.
26. Molkentin JD, Lin Q, Duncan SA, Olson EN. Requirement of the transcription factor GATA4 for heart tube formation and ventral morphogenesis. Genes Dev 11:1061–1072, 1997.
27. Hyslop L, Stojkovic M, Armstrong L, Walter T, Stojkovic P, Przyborski S, Herbert M, Murdoch A, Strachan T, Lako M. Downregulation of NANOG induces differentiation of human embryonic stem cells to extraembryonic lineages. Stem Cells 23:1035–1043, 2005.
28. Henderson JK, Draper JS, Baillie HS, Fishel S, Thomson JA, Moore H, Andrews PW. Preimplantation human embryos and embryonic stem cells show comparable expression of stage-specific embryonic antigens. Stem Cells 20:329–337, 2002.
29. Coucouvanis E, Martin GR. Signals for death and survival: a two-step mechanism for cavitation in the vertebrate embryo. Cell 83:279–287, 1995.
30. Conley B, Ellis S, Gulluyan L, Mollard R. BMPs regulate differentiation of visceral putative visceral endoderm layer with human embryonic stem-cell-derived-embryoid bodies. Biochem Cell Bio 85: 121–132, 2007.
31. Park YB, Kim YY, Oh SK, Chung SG, Ku S-Y, Kim SH, Choi YM, Moon SY. Alterations of proliferative and differentiation potentials of human embryonic stem cells during long-term culture. Exp Mol Med 40(1):98–108, 2008.
32. Bhattacharya B, Miura T, Brandenberger R, Mejido J, Luo Y, Yang AX, Joshi BH, Ginis I, Thies RS, Amit M, Lyons I, Condie BG, Itskovitz-Eldor J, Rao MS, Puri RK. Gene expression in human embryonic stem cell lines: unique molecular signature. Blood 103(8): 2956–2964, 2004.
33. Brimble S, Zeng X, Weiler DA, Luo Y, Liu Y, Lyons IG, Freed WJ, Rao MS, Robins AJ, Schulz TC. Karyotypic stability, genotyping, differentiation, feeder free maintenance and gene expression sampling in three human embryonic stem cell lines derived prior to August 9th 2001. Stem Cells Dev 3(6):585–597, 2004.
34. Carpenter MK, Rosler ES, Fisk GJ, Brandenberger R, Ares X, Miura T, Lucero M, Rao MS. Properties of four human embryonic stem cell lines maintained in a feeder-free culture system. Dev Dyn 229:243–258, 2004.
35. Mikkola M, Olsson C, Palgi J, Ustinov J, Palomaki T, Horelli-Kuitunen N, Knuutila S, Lundin K, Otonkoski T, Tuuri T. Distinct differentiation characteristics of individual human embryonic stem cell lines. BMC Dev Biol 8(6):40, 2006.
36. Osafune K, Caron L, Borowiak M, Martinez RJ, Fitz-Gerald CS, Sato Y, Cowan CA, Chien KR, Melton DA. Marked differences in differentiation propensity among human embryonic stem cell lines. Nat Biotechnol 26:313–315, 2008.
37. Plaia TW, Josephson R, Liu Y, Zeng X, Ording C, Toumadje A, Brimble SN, Sherrer ES, Uhl EW, Freed WJ, Schulz TC, Maitra A, Rao MS, Auerbach JM. Characterization of a new NIH registered variant human embryonic stem cell line BG01V. A tool for human embryonic stem cell research. Stem Cells 24(3):531–546, 2006.
38. Pal R, Ravindran G. Assessment of pluripotency and multilineage differentiation potential of NTERA-2 cells as a model for studying human embryonic stem cells. Cell Prolif 39(6):585–598, 2006.
39. Heng BC, Liu H, Rufaihah AJ, Cao T. Human embryonic stem cell (hES) colonies display a higher degree of spontaneous differentiation

when passaged at lower densities. In Vitro Cell Dev Biol Anim 42:54–57, 2006.

40. Prasad SM, Czepiel M, Cetinkaya C, Smigielska K, Weli SC, Lysdahl H, Gabrielsen A, Petersen K, Ehlers N, Fink T, Minger SL, Zachar V. Continuous hypoxic culturing maintains activation of Notch and allows long-term propagation of human embryonic stem cells without spontaneous differentiation. Cell Prolif 42:63–74, 2009.
41. Hori Y, Rulifson IC, Tsai BC, Heit JJ, Cahoy JD, Kim SK. Growth inhibitors promote differentiation of insulin-producing tissue from embryonic stem cells. Proc Natl Acad Sci U S A 99(25):16105–16110, 2002.
42. Tropepe V, Hitoshi S, Sirard C. Mak TW, Rossant J, van der Kooy D. Direct neural fate specification from embryonic stem cells: a primitive mammalian neural stem cell stage acquired through a default mechanism. Neuron 30:65–78, 2001.
43. Ramalho-Santos M, Yoon S, Matsuzaki Y, Mulligan RC, Melton DA. "Stemness": transcriptional profiling of embryonic and adult stem cells. Science 298:597–600, 2002.
44. Munozsanjuan I, Brivanlou AH. Neural induction, the default model and embryonic stem cells. Nat Rev Neurosci 3:271–280, 2002.
45. Tada S, Era T, Furusawa C, Sakurai H, Nishikawa S, Kinoshita M, Nakao K, Chiba T, Nishikawa S. Characterization of mesendoderm: a diverging point of the definitive endoderm and mesoderm in embryonic stem cell differentiation culture. Development 132:4363–4374, 2005.
46. Pal R, Khanna A. Role of hepatocyte-like cells in differentiation of cardiomyocytes from mouse embryonic stem cells. Stem Cell Dev 14(2):153–161, 2005.
47. Schultheiss TM, Xydas S, Lassar AB. Induction of avian myogenesis by anterior endoderm. Development 121:4203–4214, 1995.
48. Perea-Gomez A, Vella FD, Shawlot W, Oulad-Abdelghani M, Chazaud C, Meno C, Pfister V, Chen L, Robertson E, Hamada H, Behringer RR, Ang SL. Nodal antagonists in the anterior visceral endoderm prevent the formation of multiple primitive streaks. Dev Cell 3:745–756, 2002.
49. Vallier L, Reynolds D, Pedersen RA. Nodal inhibits differentiation of human embryonic stem cells along the neuroectodermal default pathway. Dev Biol 275:403–421, 2004.
50. Tay Y, Zhang J, Thomson AM, Lim B, Rigoutsos I. MicroRNAs to Nanog, Oct4 and Sox2 coding regions modulate embryonic stem cell differentiation. Nature 455:1124–1128, 2008.
51. Li XJ, Hu BY, Jones SA, Zhang YS, Lavaute T, Du ZW, Zhang SC. Directed differentiation of ventral spinal progenitors and motor neurons from human embryonic stem cells by small molecules. Stem Cells 26(4):886–893, 2008.
52. Yan Y, Yang D, Zarnowska ED, Du Z, Werbel B, Valliere C, Pearce RA, Thomson JA, Zhang SC. Directed differentiation of dopaminergic neuronal subtypes from human embryonic stem cells. Stem Cells 23(5): 781–790, 2005.
53. Zeng X, Chen J, Liu Y, Luo Y, Schulz TC, Robins AJ, Rao MS, Freed WJ. BG01V: a variant human embryonic stem cell line which exhibits rapid growth after passaging and reliable dopaminergic differentiation. Restor Neurol Neurosci 22:421–428, 2004.